

## Simultaneous removal of methylene blue and nickel ions in aqueous solution using natural clay

A.N. Tchakounte<sup>1</sup>, B.A. Ateba<sup>1,\*</sup>, P. Ngop Nkan, D. Dina<sup>1</sup>, J.M. Dika<sup>1</sup>, C.M. Kede<sup>1,2</sup>

<sup>1</sup>Department of Chemistry, Faculty of Science, University of Douala, P.O. Box 24175, Douala, Cameroon.

<sup>2</sup>Department of Process Engineering National Higher Polytechnic School of Douala, University of Douala, P.O. Box 2701, Douala, Cameroon.

Received 17 April 2021; Revised 01 June 2021; Accepted 03 June 2021.

**Abstract:** A natural clay was used as low-cost adsorbent for simultaneous removal of Ni(II) ions and methylene blue (MB) dye from an aqueous solution. FTIR, XRD and SEM analysis were used to characterize the adsorbent. Batch adsorption methodology was used to evaluate the effect of solution pH, initial pollutants concentration and contact time on adsorption performance. The equilibrium isotherm data was analyzed using the Langmuir, Freundlich, Temkin and Dubinin–Radushkevich (D-R) isotherm model. The Freundlich isotherm model provided the best fit to the experimental data for both pollutants as indicated by the values of the regression coefficient. The kinetic data was analyzed using pseudo-first order, pseudo-second order, Elovich equation and intraparticle diffusion rate equation. The pseudo-second-order model was found to explain the adsorption kinetics most effectively to the experimental data for both pollutants. The presence of intraparticle diffusion mechanism was indicated, although it was not the sole rate determining step. It was concluded that natural clay is an effective adsorbent for removal for simultaneous removal of Ni(II) ions and methylene blue (MB) dye from aqueous solution.

**Keywords:** Natural clay; Nickel (II); Methylene blue; Simultaneous removal; Kinetic.

### 1. Introduction

Natural water is polluted especially by industrial effluents loaded with many toxic chemical products discharged directly into the rivers, and on the earth ground [1]. This is a serious problem because heavy metals and organics dyes at high concentrations are toxic to aquatic ecosystems causing harmful effects to living organisms, plants and humans [2]. MB are widely used in the textile and dyestuff industries. These dyes are very toxic and even carcinogenic and this poses a serious hazard to aquatic living organisms. The effluents from different industries contain various dyes and are typically of high organic contents and color strength. Colored effluents decrease the transparency of water, influence photosynthesis activity, and raise the chemical oxygen demand, which hinders microbial activities of submerged organisms. High concentrations of nickel in the human's organism can cause health problems such as heart and liver damages, skin irritation, headache, dermatitis and nasal cancer [3,4]. Therefore, the removal of these two types of pollutants from industrial wastewaters is required before discharge into receiving waters in order to avoid these complications [5].

Techniques such as membrane filtration, reverse osmosis chemical precipitation, ion exchange, evaporation, solvent extraction, ion exchange and electrochemical treatment, have been employed severally to eliminate these harmful toxins from wastewater. However, most of these processes are expensive, complicated, ineffective at low metal

concentrations and inapplicable to a wide range of pollutants [6]. The adsorption technique has been found to be one of the most effective for the removal of pollutants from solution [7].

A lot of researches were carried out for the removal of single pollutants from synthetic solution using various adsorbents [8, 9]. Since, single hazardous pollutant rarely exists alone in the industrial effluents, the adsorption behavior of each pollutant was the result of competition between various pollutants present in the system.

The selection of an adsorbent depends favorably on certain factors which are use of operation, material cost, adsorption capacity, reuse potential and its ability to be regenerated after use [10]. A variety of adsorbents, including clays, zeolites, dried plant parts, agricultural waste biomass, biopolymers, metal oxides, micro-organisms, sewage sludge, fly ash and activated carbon have been used for pollutants removal. Clay minerals are important constituents of soil and they play the role of a natural scavenger for metals as water flows over soils or penetrate underground [11]. Smectite family has unique characteristics such as large specific surface area, high cation exchange capacity (CEC), low-cost, wide-spread availability, chemical and mechanical stability, layered structure, Bronsted and Lewis acidity, etc., have made the clay minerals excellent materials for adsorption [12].

The main objective of this study is the use of the smectite clay as a low-cost adsorbent for Ni(II) ions and MB from aqueous solution. This is to minimize the problem of high cost involved in the treatment of

\* Corresponding author: E-mail: [baruch.aab@gmail.com](mailto:baruch.aab@gmail.com) (B.A. Ateba)

industrial wastewaters. The clay was used without chemical modification in order to keep the process cost low. The effect of initial concentration, solution pH, contact time, were investigated. Equilibrium and kinetic parameters were also determined to help provide a better understanding of the sorption process.

## 2. Materials and methods

### 2.1. Material

The clay used in the batch experiments was collected from Sabga, in North West Cameroon region. The clay was dissolved in excess distilled water in a pretreated plastic container with proper stirring to ensure an effective dissolution. Then it was filtered through a 125  $\mu\text{m}$  sieve and the filtrate was allowed to settle for 24 h, after which excess water was decanted and the clay residue was sundried for several days, then dried in an oven at 105  $^{\circ}\text{C}$  for 4 hours. The dried clay was pulverized and then passed through mesh sieves of sizes 125  $\mu\text{m}$  to obtain the natural unmodified clay.

### 2.2. Stock solution preparation

All the reagents used in this study were of analytical grade, obtained from TRUST CHEMICAL CO. A binary stock solution of concentration 1000 mg/L of Ni(II) ions and MB was prepared by dissolving appropriate amounts of  $\text{Ni}(\text{NO}_3)_2 \cdot 6\text{H}_2\text{O}$  and MB in double distilled water. The working solutions were prepared by dilution of the stock solution with double distilled water to obtain solutions of concentration 20–100 mg/L. The pH of each solution was adjusted to the required value by the addition of 0.1 M NaOH or 0.1 M HCl before the adsorbent was added.

### 2.3. Adsorbent characterization

The specific surface area of the clay is determined by the Brunauer Emmet Teller (BET) method. Elemental analysis was determined by wet chemical method and measurement of elemental concentration was done by using an atomic absorption spectrophotometer (AAS) supplied by PerkinElmer, USA, Model Analyst 700. Scanning electron microscopy (SEM) investigations of the clay samples were conducted in a JEOL JMT-300 operated at 30 kV and linked with an energy dispersive X-ray spectrometry (EDXS) attachment. The SEM analysis was done at 1000 $\times$  magnification. X-ray diffraction (XRD) analysis was determined using a model MD 10 Randicon diffractometer operating at 25 kV and 20 mA. The scanning regions of the diffraction were 16–72 $^{\circ}$  on the 2 $\theta$  angle. The Fourier transform infra-red (FTIR) spectroscopic technique was utilized to identify the functional groups of the adsorbent. The pH point of zero charge or  $\text{pH}_{\text{pzc}}$  was determined based on the method described [13].

### 2.4. Adsorption procedure

The adsorption was carried out in 100 mL pretreated plastic bottles at an adsorbent dose of 0.2 g, metal and

dye concentration of 100 mg/L, adsorbent particle size 125  $\mu\text{m}$ , and contact time of 30 min. This was done by reacting 0.2 g of the natural clay with 30 mL of the adsorbate. The effect of pH was carried out at pH values of 2–10. The influence of initial metal ion concentration was carried by varying the adsorbate concentration from 20 to 100 mg/L. The effect of contact time was conducted by varying the contact time from 5 to 30 min. The residual concentration of MB and Ni(II) ions was determined using Spectroquant Pharo 300 spectrophotometer.

The quantity of a pollutant adsorbed from the solution was calculated by:

$$Q = \frac{(C_0 - C_t) \cdot V}{m} \quad (1)$$

where V is the volume (L), m is the mass of clay (g),  $C_0$  is the initial concentration of pollutant (mg/L) and  $C_t$  is the concentration of pollutant at a time t.

## 3. Results and discussion

### 3.1. Adsorbent characterization

The physicochemical analysis of clay is presented in Table 1. The mineral analysis of clay showed that the most abundant oxides are  $\text{SiO}_2$ ,  $\text{Al}_2\text{O}_3$  and  $\text{Fe}_2\text{O}_3$  whereas  $\text{K}_2\text{O}$ ,  $\text{CaO}$ ,  $\text{Na}_2\text{O}$ ,  $\text{MgO}$ ,  $\text{TiO}_2$  and  $\text{MnO}$  are present only in small quantities. The  $\text{SiO}_2/\text{Al}_2\text{O}_3$  ratio is greater than 5 for the sample owing to its sandy content.  $\text{Fe}_2\text{O}_3$  content is > 5%. The  $\text{Na}_2\text{O}$  (0.21%) and  $\text{K}_2\text{O}$  (0.44%) contents can be related to the presence of minor amounts of Na/K-feldspars.

The adsorption-desorption isotherm of  $\text{N}_2$  onto the natural clay is represented in Fig.1. The isotherm of clay is of type IV, characteristic of a multi-layer adsorption with a medium slightly porous structure. This result is confirmed by SEM micrograph on Fig.2. These isotherms show a hysteresis resulting from capillary condensation. The form of this hysteresis indicates to the presence of the pores in bottles with a neck a little lower than the body. These broad loops of hysteresis are due to the presence of cracks or of slits in which the molecules of nitrogen do not desorb in the same way than they were adsorbed in multi-layer adsorption. SEM analysis is another important tool used in the determination of the surface morphology of an adsorbent. The SEM images of natural clay at sizes of 100  $\mu\text{m}$ , 20  $\mu\text{m}$  and 10  $\mu\text{m}$  is shown in Fig.2. The examination of SEM micrographs of natural clay shows that this material is presented in the form of plates. These micrographs also show that the clays are made of variable cluster of different sizes with a prevalence of spherical particles. SEM micrographs of the studied clay present homogeneous surfaces. The XRD spectrum of natural clay in Fig.3 gives information about the changes in the crystal line and amorphous or crystalline nature of the adsorbent. XRD spectrum of clay shows a material predominantly amorphous with some minor crystalline characteristics. Some minerals could be identified with more or less safety (Fig.3): Quartz  $\text{SiO}_2$ ,

Anorthoclase  $(\text{Na,K})(\text{Si}_3\text{Al})\text{O}_8$ , Anorthite  $(\text{Ca,Na})(\text{Al,Si})_2\text{Si}_2\text{O}_8$ , Muscovite  $\text{KAlSi}_3\text{AlO}_{10}(\text{OH})_2$  and illite  $\text{KAl}_2(\text{Si}_3\text{Al})\text{O}_{10}(\text{OH})_2$ . The FT-IR spectrum of clay is shown in Fig.4 frequency absorption band at  $3688.38\text{ cm}^{-1}$  (OH-Al out-of-plane),  $3620.39\text{ cm}^{-1}$  (OH-Al in-plane) and  $911.15$  indicates the presence of OH-Al groups [14]. The bands appearing at  $1115.68$  and  $1003.45\text{ cm}^{-1}$  are ascribed to the formation of Si-O bond, characteristic of aluminosilicate [15]. The additional peak at  $679.77\text{ cm}^{-1}$  indicates the presence of Al-OH and Si-O [15]. The bands observed at  $468.88$  and  $540\text{ cm}^{-1}$  could be attributed to vibrations due to deformation of Si-O and Si-O-Al bonds, respectively [16].

### 3.2 Influence of initial pH

In each study of adsorption of pollutants, the pH is the most important parameter. The pollutants uptake is

strongly dependent on the pH. The effect of pH on the simultaneous removal of Ni(II) and MB unto clay is shown in Fig.5. As it can be seen from the curves plotted, the maximum removal capacity of both pollutants is at around pH 6. The  $\text{pH}_{\text{pzc}}$  of natural clay is 5.6. the overall surface charge is positive for solution pH lower than this value and it is negative when the pH is higher than  $\text{pH}_{\text{pzc}}$ . MB dye used is basic, its dissolution in water releases positively charged colored ions. The retention of both pollutants increases with increasing negative surface charge. This explains why the retention is more remarkable when the pH exceeds the values of 6. However, this loss of efficiency, as pH increases shows that the retention is rather complex and far from being a simple electrostatic attraction between opposite charged species.

**Table 1**

Major elemental compositions of the natural clay

Chemical composition (weight %)	SiO <sub>2</sub>	Al <sub>2</sub> O <sub>3</sub>	Fe <sub>2</sub> O <sub>3</sub>	K <sub>2</sub> O	CaO	Na <sub>2</sub> O	MgO	TiO <sub>2</sub>	MnO	P <sub>2</sub> O <sub>5</sub>	LOI	Total	SiO <sub>2</sub> /Al <sub>2</sub> O <sub>3</sub>
	68.23	13.57	6.60	0.44	0.68	0.21	0.44	0.21	0.01	<L.D	10.51	100.91	5.03

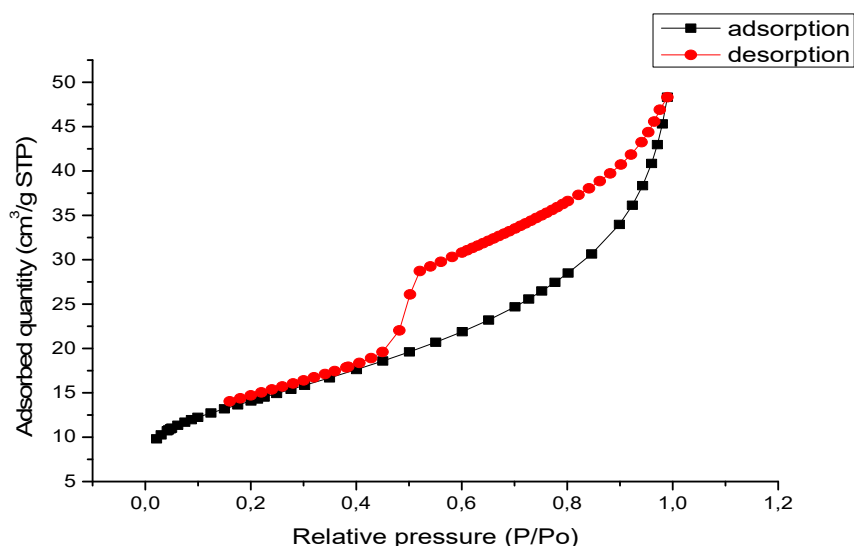


**Fig.1.** N<sub>2</sub> adsorption-desorption isotherm of natural clay

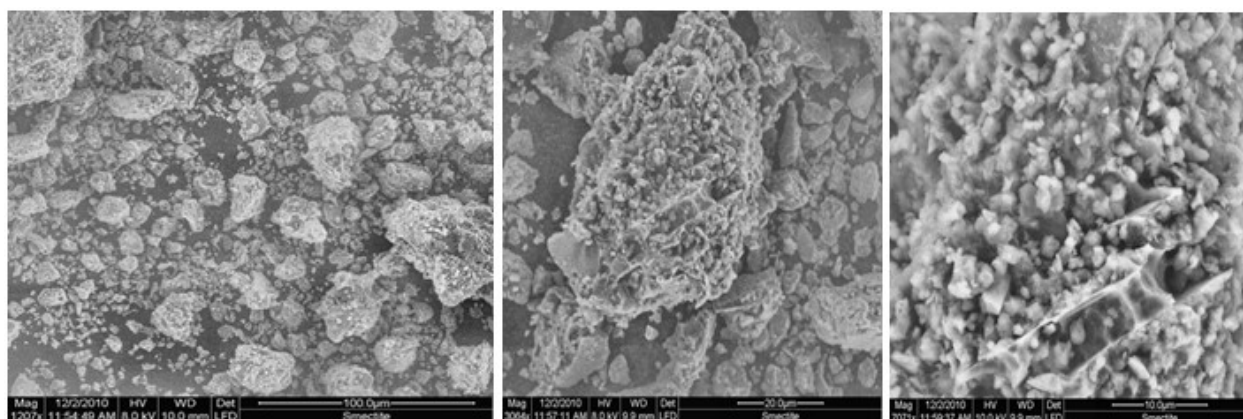


**Fig.2.** SEM micrograph of the natural clay

### 3.3 Effect of initial concentration

The adsorption rate of metal ions into adsorbents is a function of the initial concentration of the metal ions which makes it an important factor to be determined for an effective sorption. The effect of initial metal ion concentration on the adsorption of Ni(II) ions and MB into natural clay is shown in Fig.6. It was observed that the adsorption capacity of both pollutants increases with increase initial concentration of pollutant. This is a result of the increasing concentration gradient which acts like a driving force to overcome the resistance to mass transfer of pollutants between the adsorbate and adsorbent species [17].

### 3.4 Effect of contact time

The time necessary to reach the equilibrium of adsorption of Ni (II) and MB onto natural clay was investigated at initial concentration of 60 mg/L. The effect of contact time on the adsorption capacity of Ni(II) and MB into natural clay is presented in Fig.7. It is observed that the rate of removal of both pollutants from solution was initially quick and then slowed gradually until an equilibrium time beyond which there was no significant increase in the removal rate. Equilibrium removal was achieved around 30 min and increased slightly up to 45 min for both pollutants. Hence, a contact time of 30 min was chosen to ensure optimum removal of pollutants.

A large number of vacant active sites are occupied by the ions during the initial time of contact. After a period of time, the vacant surface sites are difficult to be available because of the repulsive forces between the pollutants adsorbed on the clay surface and the ions in solution. Therefore, the mesopores of the surface of clay minerals were saturated with pollutants in the initial stage of adsorption. Thereafter, the pollutants have to traverse farther and deeper into the pores encountering much larger resistance. And result was the slow adsorption during the later period of adsorption [18].

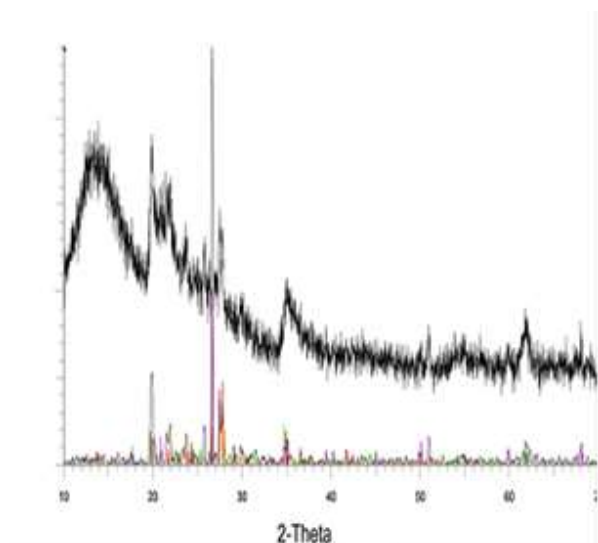


Fig.3. XRD pattern of natural clay

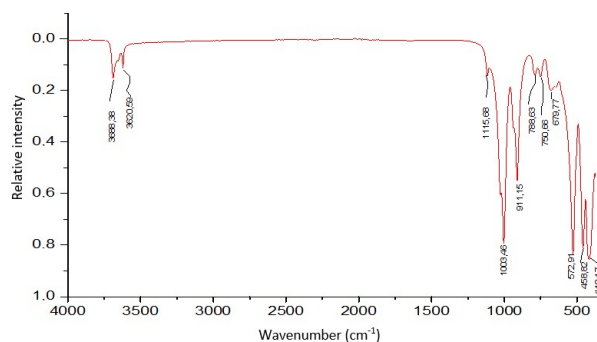


Fig.4. Infrared spectra of natural clay

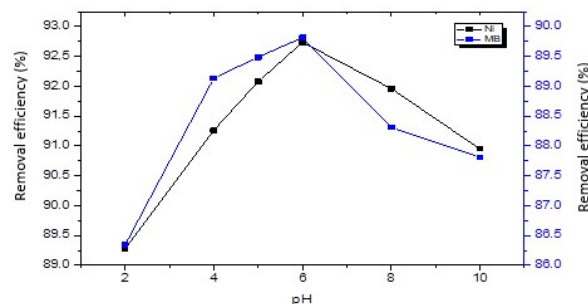


Fig.5. The effect of initial pH of solution on the removal efficiency of Ni(II) and MB from solution by natural clay

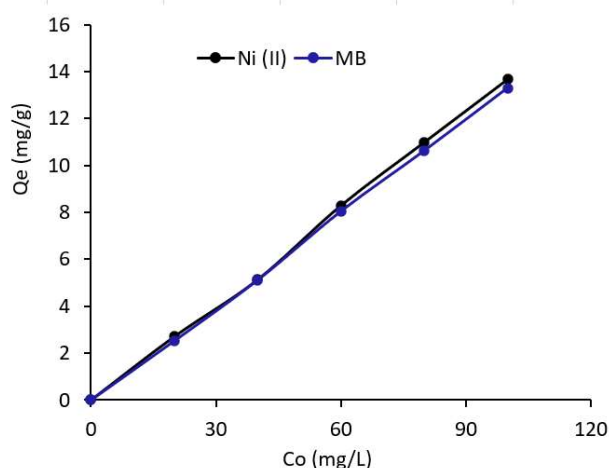


Fig.6. The effect of initial pollutant concentration on the adsorption uptake capacity of clay for Ni (II) ions and MB

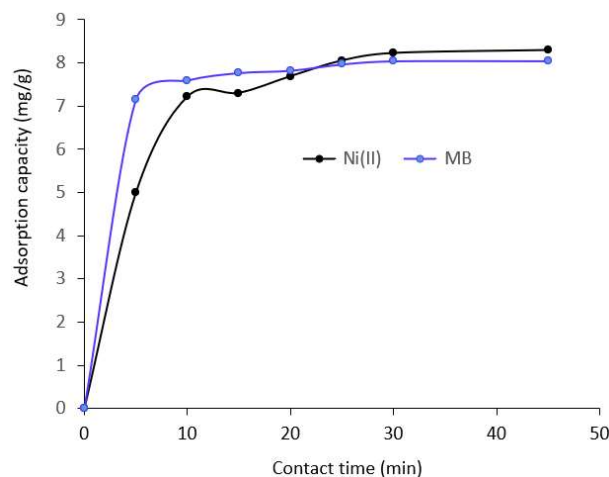


Fig.7. The effect of contact time on the adsorption uptake capacity of clay for Ni (II) ions and MB



### 3.5 Kinetic study

The mechanism of the adsorption process depends on the physical and chemical characteristic of the adsorbent and adsorbate. In order to investigate the kinetics adsorption of MB and Ni(II) ions, the Lagergren-first-order, pseudo-second-order, Elovich kinetic models and intraparticle diffusion model [19] were used.

The pseudo-first order rate equation was proposed by Lagergren and is widely used for the adsorption of liquid/solid system [20]. The linear form of Lagergren equation is generally expressed as:

$$\log(q_e - q_t) = \log q_e - \frac{k_1 t}{2.303} \quad (2)$$

where  $k_1$  ( $\text{min}^{-1}$ ) is pseudo-first order rate constant at equilibrium.  $q_e$  and  $q_t$  are adsorption uptake of adsorbate at equilibrium and at time  $t$ (min), respectively.

Pseudo-second order model [21] suggests that both number of adsorption sites on the material surface and concentration of adsorbate ions in the liquid phase determine the rate. The linearized form of model is:

$$\left(\frac{t}{q_t}\right) = \left(\frac{t}{q_e}\right) + \left(\frac{1}{k_2 q_e^2}\right) \quad (3)$$

where  $h = k_2 q_e^2$  and  $k_2$  are initial and overall rate constants for adsorption which can be calculated from slope and intercept of plot  $t/q_t$  vs  $t$ .

Elovich kinetic relationship, developed by is suitable to describe second order kinetics assuming that the actual solid surfaces are energetically heterogeneous [22]. The mathematical relationship in linearized form is:

$$q_t = \left(\frac{1}{\beta}\right) \ln(\alpha\beta) + \left(\frac{1}{\beta}\right) \ln t \quad (4)$$

where  $\alpha$ (mg/g.min) is the initial adsorption rate and  $\beta$ (g/mg) is related to the extent of surface coverage and activation energy for chemisorption.

Once adsorbed on the surface, solute particles diffuse into the pores on the surface of adsorbent and form bonding, which may be the rate determining step [22] Weber and Morris intraparticle diffusion model is given by:

$$q_t = k_d t^{1/2} + I \quad (5)$$

where  $k_d$  (mg/g.min<sup>1/2</sup>) is the rate constant for intraparticle diffusion  $k_d$  can be found from slope of plot  $\ln(q_t)$  vs  $\ln(t)$  and  $I$  is the intercept. For an absorbing system the straight line should pass through the origin and the intercept value provides an idea about the deviation from intraparticle diffusion model or contribution of the film diffusion mechanism [23].

From Table 2, it is seen that the pseudo-first order equation provided a good fit to the experimental data of both pollutants. This is indicated by the high values of their linear regression ( $R^2$ ) close to 1.

The calculated adsorption capacity values from the pseudo-second order model are in a good agreement with those experimentally determined. Moreover, the correlation coefficient values are quite well  $> 0.999$ , and

much higher than those found by the pseudo-first order kinetic model. Thus, we can assert that the adsorbent systems are well described by the pseudo-second order kinetic model.

The adsorption data was also analyzed using the Elovich equation. From Table 2, the correlation coefficient of both Ni(II) ions and MB are lower than pseudo first and pseudo-second order models, the Elovich kinetic model did not provide a good fit to the experimental data.

Intraparticle diffusion model is given by equation (5). As indicated in table 3, the presence of the intercept ( $I$ ), it shows that the plots did not pass through the origin but were close to it. This deviation from the origin is due to the difference in the rate of mass transfer in the initial and final stages of the adsorption process [24].

**Table 2**

Comparison of the kinetic model equations on the adsorption of Ni(II) ions and MB(II) from solution unto natural clay

Kinetic models	Ni(II)	MB
<b>Pseudo-first order</b>		
$k_1$ ( $\text{min}^{-1}$ )	0.144	0.207
$R^2$	0.961	0.880
<b>Pseudo-second order</b>		
$q_{\text{ecal}}$ (mg/g)	8.968	8.196
$h$ (mg/g min)	2.800	10.482
$k_2$ (g/mg.min)	0.034	0.156
$R^2$	0.998	0.999
<b>Elovich equation</b>		
$\alpha$ (mg/g.min)	8.858	2110.26
$\beta$ (g/min)	0.344	1.192
$R^2$	0.870	0.841
<b>Intraparticle diffusion</b>		
$k_d$ (mg/g.min <sup>1/2</sup> )	1.072	1.230
$I$	2.650	1.712
$R^2$	0.655	0.827

### 3.6 Adsorption isotherm

Adsorption isotherm expresses the relationship between the amount of adsorbate removed from the liquid phase by unit mass of adsorbent at a constant temperature. Adsorption isotherms are basic requirements for the design of adsorption systems. A precise mathematical description of equilibrium adsorption capacity is very important for reliable prediction of adsorption parameters and quantitative comparison of adsorption behavior for different adsorbent systems. The parameters of equilibrium isotherms often give useful information on sorption mechanism, surface properties and affinity of the adsorbent. It is therefore important to determine the most suitable correlation of equilibrium curves in order to optimize the conditions for designing adsorption systems [25]. In this study, the Langmuir, Freundlich, Temkin and Dubinin-Radushkevich (D-R) isotherms were tested to analyze the equilibrium data, and the results are shown in Table 3.

The Langmuir sorption isotherm has been successfully applied to many pollutant biosorption processes and has been the most widely used isotherm for the biosorption of a solute from a liquid solution. A basic assumption of the Langmuir theory is that sorption takes place at specific homogeneous sites within the sorbent. This model can be written in linear form [26]:

$$\frac{C_e}{Q_e} = \frac{1}{K_L Q_{max}} + \frac{1}{Q_{max}} C_e \quad (6)$$

where  $Q_e$  is the equilibrium concentration on the adsorbent (mg/g),  $C_e$  is the equilibrium concentration in the solution (mg/L),  $Q_{max}$  is a maximum adsorption capacity of the adsorbent (mg/g), and  $K_L$  is the monolayer adsorption capacity of the Langmuir adsorption constant (L/mg) related with the free energy of adsorption. Fig.8 and Table 3 indicates the linear relationship between the amount (mg) of both pollutants adsorbed per unit mass (g) of natural clay against the concentration of pollutants remaining in solution (mg/L). The correlation coefficient ( $R^2$ ) of both pollutants are very low, 0.5534 and 0.0050, indicating a poor fit of the monolayer Langmuir isotherm to the adsorption of Ni(II) and MB by natural clay.

The essential features of the Langmuir isotherm can be expressed in terms of a dimensionless constant separation factor ( $R_L$ ) defined by the relationship [27]:

$$R_L = \frac{1}{(1 + K_L C_0)} \quad (7)$$

where  $C_0$  is the initial metal ion concentration in (mg/L) and  $K_L$  is the Langmuir equilibrium constant (L/mg). The value of the separation factor provides important information about the nature of the adsorption process. The adsorption is said to be irreversible ( $R_L = 0$ ), favorable ( $0 < R_L < 1$ ), linear ( $R_L = 1$ ) or unfavorable ( $R_L > 1$ ). For the initial pollutants concentration from 20 to 100 mg/L for Ni(II) ions and MB used in this study, the values of  $R_L$  ranged from 0.30 to 0.67. This indicates a favorable adsorption of metal ions and dye onto natural clay.

The Freundlich isotherm model is applied to non-ideal sorption on heterogeneous surfaces and the linear form of the equation is given [23]:

$$\log Q_e = \log K_F + \frac{1}{n} \log C_e \quad (8)$$

where  $K_F$  is a constant relating the adsorption capacity and  $1/n$  is a parameter relating the adsorption intensity, which varies with the heterogeneity of the material (Fig.9 and Table 3). The values of  $n$  indicate that the type of adsorption is favorable in the range of 2-10, moderate in the range of 1-2 and poor if  $n < 1$  [28].

As can be seen from Table 3 and Fig.9, the values of the correlation coefficient ( $R^2$ ) is 0.8263 for Ni(II) and 0.9599 for MB. Thus, the Freundlich isotherm gave a better fit to the data than the Langmuir isotherm model for both pollutants. The higher  $R^2$  of the Freundlich model implied a greater tendency of the heterogeneous surface of natural clay [29] for the removal of Ni(II) and MB. The value of  $n$  obtained is 0.9749 and 0.7499 for

Ni(II) and MB respectively, indicating a unfavorable adsorption process.

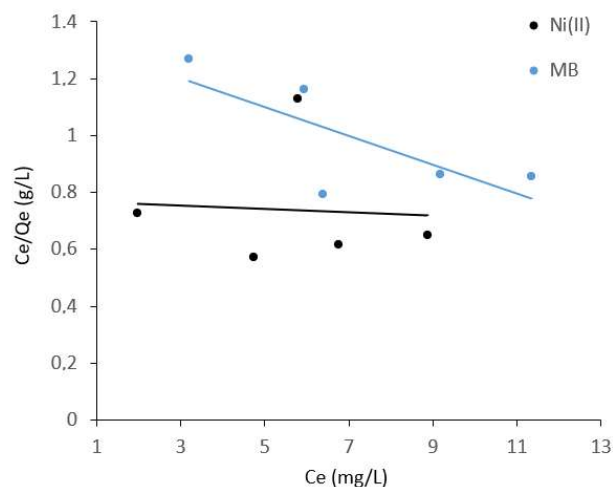


Fig.8. Langmuir adsorption isotherm for removal of Ni(II) ions and MB onto natural clay

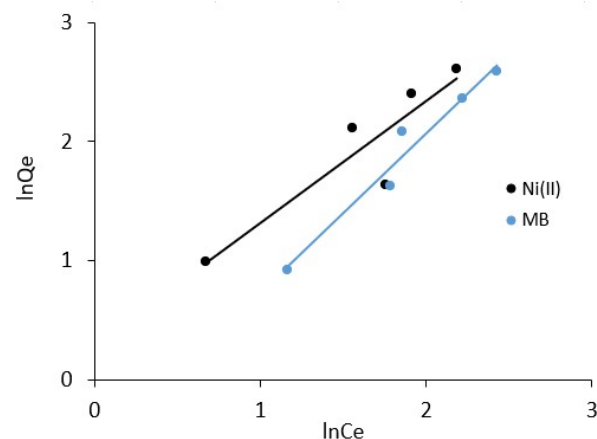


Fig.9. Freundlich adsorption isotherm for removal of Ni(II) ions and MB onto natural clay

The Temkin isotherm contains a factor that explicitly takes into account of the adsorbent-adsorbate interactions. In this equation, it is assumed that, because of these interactions and ignoring very low and very large concentration values, the heat of adsorption of all molecules in the layer would decrease linearly with the coverage [30]. The linear form of the Temkin model is written as:

$$Q_e = B \ln A + B \ln C_e \quad (9)$$

where  $B = RT/b_T$ ,  $T$  is the temperature (K),  $R$  is the ideal gas constant (8.314 J/mol.K) and  $A$  and  $b_T$  are constants. The constant  $B$  is related to the heat of adsorption and  $A$  is the equilibrium binding constant (L/mg) corresponding to the maximum binding energy. The correlation coefficients  $R^2$  of 0.8112 for Ni(II) and 0.9620 for MB are lower than that of the Freundlich isotherm model, although better than the Langmuir isotherm. Therefore, the adsorption of both pollutants into natural clay does not fit the Temkin isotherm as well as the Freundlich isotherm does.

To distinguish between physical and chemical adsorption, the adsorption data can be further interpreted by Dubinin-Radushkevich (D-R) isotherm [31]. This isotherm is more general than Langmuir isotherm because it does not assume a homogenous surface or a constant adsorption potential [32]. The linear form of the D-R isotherm model is written as:

$$\ln Q_e = \ln Q_m - \beta \varepsilon^2 \quad (10)$$

Where  $\beta$  is the coefficient related to the mean free energy of adsorption per mol of the adsorbate ( $\text{mol}^2/\text{J}^2$ ),  $q_m$  is the theoretical saturation capacity ( $\text{mg/g}$ ) and  $\varepsilon$  is the Polanyi potential expressed as:

$$\varepsilon = RT \ln \left( 1 + \frac{1}{C_e} \right) \quad (11)$$

The D–R parameters  $\beta$  and  $q_m$  are calculated from the intercept and the slope of the line in Fig.11, respectively, and the values are given in Table 3. The mean free energy of adsorption defined as the free energy change when 1 mol of ion is transferred to the surface of the solid from infinity in solution [33] was calculated from  $\beta$  values (Table 3). It is known that magnitude of  $E$  is useful for estimating the type of adsorption and if this value is between 8 and 16 kJ/mol, the adsorption type can be explained by ion exchange [34].

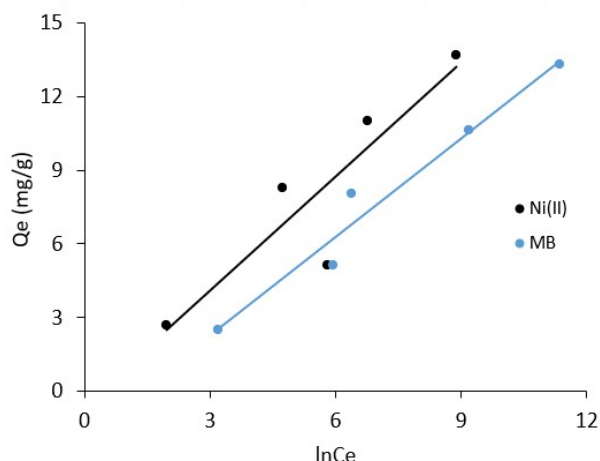


**Fig.10.** Temkin adsorption isotherm for removal of Ni(II) ions and MB onto natural clay

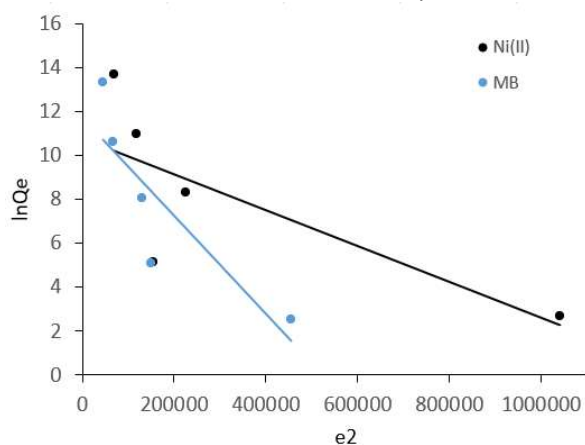


**Fig.11.** D-R adsorption isotherm for removal of Ni(II) ions and MB onto natural clay

**Table 3**

A comparison of the Langmuir, Freundlich, Temkin and Dubinin-Radushkevich isotherm constants for the adsorption of Ni (II) ions and MB into natural clay

Isotherm models	Ni(II)	MB
Langmuir model		
$q_m$ (mg.g)	19.920	158.73
$K_L$ (L/mg)	0.037	0.008
$R^2$	0.553	0.005
Freundlich model		
$K_F$ (mg/g) ( $\text{mg/L}$ ) $^{1/n}$	1.342	0.548
$n$	0.974	0.749
$R^2$	0.826	0.959
Temkin model		
$B$ (mg/g)	1.550	1.336
$A$ (L/g)	0.696	0.276
$R^2$	0.811	0.962
Dubinin–Radushkevich model		
$q_m$ (mg/g)	48.580	116.42
$\beta$ ( $\text{mol}^2/\text{kJ}^2$ )	$8 \times 10^{-6}$	$20 \times 10^{-6}$
$R^2$	0.571	0.741

#### 4. Conclusion

In this work, the removal of nickel ions and methylene blue dyes from aqueous solution into natural clay has been investigated. The adsorption results showed that the natural clay is an effective absorbent for removal nickel ions and methylene blue dyes with high adsorption uptake under the optimum operating condition: 30 min contact time and pH= 6. The maximum adsorption quantity to natural clay increase in the order: MB < Ni(II). The equilibrium data were tested using the Langmuir, Freundlich, Temkin and Dubinin-Radushkevich (D-R) isotherm model and the best fit was obtained with the Freundlich model. Kinetic parameters were also analyzed using the Lagergren pseudo-first order, pseudo-second order, Elovich equation and intraparticle diffusion rate equation. The pseudo-second order equation provided the best fit to the experimental data and the result also indicated the presence of intraparticle diffusion on the sorption of both metal ions, although it was not the sole rate determining step.

#### Conflicts of interest

The authors declare no conflicts of interests.

#### References

- [1] N. Unlu, M. Ersoz, Journal of Hazardous Materials 136(2) (2006) 272–280.
- [2] S.S. Ahluwalia, D. Goyal, Bioresource Technology 98(12) (2007) 2243–2257.
- [3] S. Wang, X. Shi, Molecular and Cellular Biochemistry 222 (2001) 3–9.
- [4] E. Denkhau, K. Salnikow, Critical Reviews in Oncology/Hematology 42(1) (2002) 35–56.

- [5] M. Sprynskyy, B. Buszewski, A.P. Terzyk, J. Namiesnik, *Journal of Colloid and Interface Science* 304 (2006) 21-28.
- [6] T.K. Kurniawan, G.Y.S. Chan, W. Lo, S. Babel, *Science of The Total Environment* 366 (2006) 409-426.
- [7] S. Liang, X. Guo, N. Feng, Q. Tian, *Journal of Hazardous Materials* 174 (2009) 756-762.
- [8] F. Boudrahem, F. Aissani-Benissad, A. Soualah, *The Journal of Chemical & Engineering Data* 56 (2011) 1804-1812.
- [9] Y.S. Al-Degs, M.I. El-Barghouthi, A.A. Issa, M.A. Khraisheh, G.M. Walker, *Water Research* 40 (2006) 2645-2658.
- [10] K.S. Obayomi, M. Auta, *Heliyon* 5 (2019) e02799.
- [11] K.G. Bhattacharyya, S.S. Gupta, *Applied Clay Science* 41 (2007) 1-9.
- [12] A. Soliemanzadeh, M. Fekri, *Chinese journal of chemical engineering* 25 (2017) 924-930.
- [13] M.S. Onyango, Y. Kojima, O. Aoyi, E.C. Bernardo, H. Matsuda, *Journal of Colloid and Interface Science* 279 (2004) 341-50.
- [14] Z-X. Chen, X-Y. Jin, Z. Chen, M. Megharaj, R. Naidu, *Journal of Colloid and Interface Science* 363 (2011) 601-607.
- [15] S.S. Amritphale, S. Bhasin, N. Chandra, *Ceramics International* 32(2) (2006) 181-187.
- [16] H. Sayilkan, S. Erdemoglu, S. Sener, F. Sayilkan, M. Akarsu, M. Erdemoglu, *Journal of Colloid and Interface Science* 275 (2004) 530-538.
- [17] B. Das, N.K. Mondal, *Clean Technologies and Environmental Policy* 18 (2016) 867-881.
- [18] A.A. Rouff, E.J. Elzinga, R.J. Reeder, N.S. Fisher, *Environmental Science & Technology* 40 (2006) 1792-1798.
- [19] A.N. Tchakounte, H.Z. Poumve, C.M. Kede, J.M. Dika, *Journal of Applied Surfaces and Interfaces* 6(1-3) (2019), 9-17.
- [20] B. Kakavandi, R.R. Kalantary, M. Farzadkia, A.H. Mahvi, A. Esrafil, A. Azari, A.R. Yari, A.B. Javid, *Journal of Environmental Health Science & Engineering* 12 (2014) 115.
- [21] C.M. Kede, P.P. Ndibewu, M.M. Kalumba, N.A. Panichev, H.M. Ngomo, J.M. Ketcha, *South African Journal of Chemistry* 68 (2015) 226-235.
- [22] M. Ghaedi, H. Mazaheri, S. Khodadoust, S. Hajati, M.K. Purkait, *Spectrochimica Acta Part A: Molecular and Biomolecular Spectroscopy* 135 (2015) 479-490.
- [23] P.P. Ndiehu, C.M. Kede, P.G. Tchieta, H.Z. Poumve, A.N. Tchakounte, *Journal of applied Surface and Interfaces* 5(1-3) (2019), 21-30.
- [24] B. Das, N.K. Mondal, *Universal Journal of Environmental Research and Technology* 1(4) (2011) 515-530.
- [25] J.C.P. Vaggetti, E.C. Lima, B. Roger, J.L. Brasil, B.M. Da Cunha, N.M. Simon, N.F. Cardoso, C.P. Zapata Noreña, *Biochemical Engineering Journal* 42 (2008) 67-76.
- [26] E. Igberase, P. Osifo, A. Ofomaja, *Journal of environmental chemical engineering* 2 (2014) 362-369.
- [27] T.-S. Anirudhan, P.G. Radharishnan, *The Journal of Chemical Thermodynamics* 40 (2008) 702-709.
- [28] B.H. Hameed, D.K. Mahmoud, A.L. Ahmad, *Journal of Hazardous Materials* 158(1) (2008) 65-72.
- [29] M. Hua, S. Zhang, B. Pan, W. Zhang, L. Lv, Q. Zhang, *Journal of Hazardous Materials* 211-212 (2012) 317-331.
- [30] H. Lalhrualuanga, K. Jayaram, M.N.V. Prasad, K.K. Kumar, *Journal of Hazardous Materials* 175(1-3) (2010) 311-318.
- [31] K. Adebawale, B. Olu-Owolabi, E. Chigbundu, *Journal of Encapsulation and Adsorption Science*, 4 (2014), 89-104.
- [32] A. Kilislioglu, B. Bilgin, *Applied Radiation and Isotopes* 58(2) (2003) 155-160.
- [33] M.S. Onyango, Y. Kojima, O. Aoyi, E.C. Bernardo, H. Matsuda, *Journal of Colloid and Interface Science* 279(2) (2004) 341-350.
- [34] A.A.M. Daifullah, S.M. Yakout, S.A. Elreefy, *Journal of Hazardous Materials*. 147 (2007) 633-643.